



ELSEVIER

International Journal of Mass Spectrometry 189 (1999) 115–123



Laser ablation of graphite at 355 nm: cluster formation and plume propagation

Young-Ku Choi^a, Hoong-Sun Im^b, Kwang-Woo Jung^{a,*}

^aDepartment of Chemistry, Wonkwang University, Iksan 570-749, Korea

^bKorea Research Institute of Standards and Science, Taeduk Science Town, Taejeon 305-600, Korea

Received 17 December 1998; accepted 6 April 1999

Abstract

Ablation dynamics of C_n^+ ions ejected from a 355-nm laser ablation of graphite target in vacuum has been investigated by time-of-flight (TOF) mass spectrometry. At 0.5 J/cm² laser fluence, the larger cluster ions are predominantly produced. With increasing laser fluence, however, the maximum size distribution moves toward small cluster ions. A strong nonlinear dependence of the amount of desorbed C_n^+ cluster ions on laser fluence is observed under moderate laser fluence conditions (≤ 1 J/cm²). This is interpreted by the mechanism that C_n^+ ions are produced directly from the graphite via conversion of the multiphoton energy into thermal energy. The time resolved analysis of the ablated C^+ ions shows the two drift velocities with the fast and slow components. The result indicates that the ejecta emitted above the target surface separates into two components during plume propagation. (Int J Mass Spectrom 189 (1999) 115–123) © 1999 Elsevier Science B.V.

Keywords: Graphite; Laser ablation; Time-of-flight (TOF) mass spectrometry

1. Introduction

The laser ablation technique has marked significant progress in its application to many fields of material process such as production of microclusters, growth of thin films, annealing, etching, and chemical modification of surface layers in the fabrication of micro-electronic devices [1]. Recently, the pulsed laser ablation of a graphite target has proved to be a powerful tool for the preparation of newly found materials like fullerenes [2], single-walled nanotubes [3], and diamondlike carbon (DLC) films [4]. The study of carbon clusters is particularly interesting

because of the clusters' fascinating structural and spectroscopic properties, their importance in astrophysical processes, and their role in combustion and soot formation.

Carbon clusters have been thought to grow through the aggregation of the species vaporized from the graphite [2,5]. Bloomfield et al. [6] and Cox et al. [7] have reported an alternative pathway of the carbon cluster formation. They have suggested that the carbon clusters are most likely formed via fragmentation of the initially formed larger clusters and laser-desorbed carbon dust. In recent studies on the mass distribution of neutral carbon clusters generated by laser vaporization of graphite in He, Achiba et al. [8,9] have also reported that the carbon clusters originated from the large hot clusters that lead to

* Corresponding author. E-mail: kwjung@wonnm.wonkwang.ac.kr

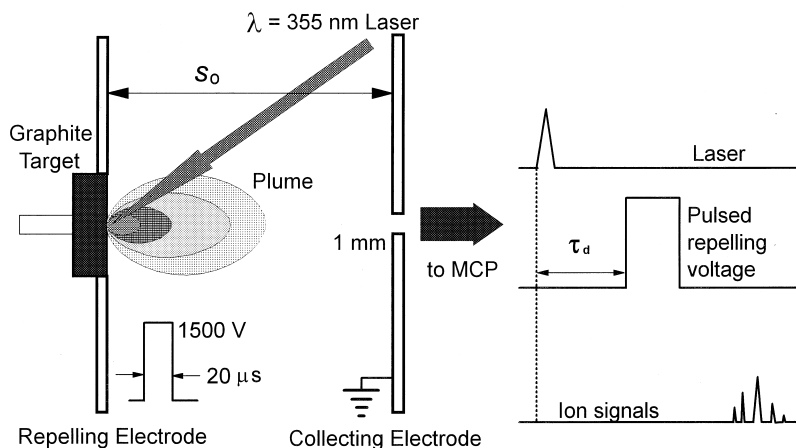


Fig. 1. Diagram of experimental setup for pulsed-field time-of-flight mass spectrometry.

fragmentation into these smaller clusters. In spite of extensive studies during the last decade, there still remain many problems to be unraveled, not only from the viewpoint of understanding the chemical and physical properties of carbon clusters, but also in clarifying the formation mechanism of these species.

The temporal velocity profile of ejected materials is an important characteristic in the production of reactive species and for determining the structural quality of the deposited film because the kinetic energy of the species is a key controlling parameter [10,11]. Although laser-ablated plasmas have been studied to some extent, the dynamics of laser interaction with materials as well as the detailed aspects of laser-induced plume formation and expansion are not fully understood, particularly in the case of carbon. Studying the spatial and velocity distribution of the ablated species, particularly during initial ejection and expansion, can provide a better understanding of the ablation dynamics.

This article presents a study of the mass distribution of positive carbon-cluster ions generated by laser ablation of graphite at a wavelength of 355 nm. The laser-induced plume from the graphite target in a high vacuum condition is characterized by measuring its time-of-flight mass spectra (TOFMS) with varying laser fluence. The fluence dependence of the observed C_n^+ signals is discussed on the basis of the energetics of cluster formation and the fragmentation process.

The flow dynamics of plume expansion are also investigated by the pulsed-field time-of-flight mass spectrometric technique.

2. Experimental

Fig. 1 shows an experimental setup containing a graphite target and the ion-accelerating electrodes of the single-stage TOFMS. Laser ablation of a graphite target was carried out in a vacuum chamber (base pressure $<5 \times 10^{-7}$ Torr) combined with a TOFMS, where positive ions were accelerated by an electric field, applied to the repelling electrode, and detected with a microchannel plate (MCP) detector. A target disk (10 mm in diameter, 2.5 mm thick) of graphite (99.95% purity, Goodfellow Metals Ltd.) was placed at the repeller of the ion optics. The third harmonic output (355 nm) of an Nd:YAG laser (10 ns pulse width), operated at a repetition rate of 10 Hz, strikes the solid target at an incident angle of $\sim 45^\circ$ with respect to the target normal. The radiation was focused by a 50 cm focal length lens to a spot size of $3 \times 10^{-2} \text{ cm}^2$. The laser fluence at the target surface was varied in the range 0.5–1.0 J/cm².

The ablated materials evolve in the region between the repelling and the collecting electrodes. Following a delay of typically $\tau_d = 0\text{--}1.0 \text{ } \mu\text{s}$ after the laser shot, the positive ions are extracted by a +1500 V

pulsed electric field, applied to the repeller, and enter the small orifice, 1 mm in diameter, of the collecting electrode. The ion extraction pulse has a rise time of 40 ns and duration of 20 μ s. The ions are then moved toward the ion detector through the field-free drift tube. The overall flight path length is about 162 cm including the extracting distance S_0 of 1 cm.

The TOF mass spectrometer can be operated in the following two modes, depending on the delay time of the pulsed repelling field: (1) mass spectrometer mode, and (2) translational spectrometer mode. In the first mode, the ions are accelerated without delay time ($\tau_d = 0$) immediately after the laser ablation, thus the mass spectrum can be obtained. In the second mode, the velocity distribution of the ablated ions can be determined by measuring its TOF distribution at a variable τ_d with respect to the timing of the laser pulse. Because the ions in the ejected plume propagate in the field-free region of the source during the delay time τ_d , the velocity components at directions normal to the ablation surface can be calculated from the arrival time of ion, the delay time τ_d , and the geometric parameters of the mass spectrometer. Details will be given in a forthcoming publication [12]. This method thus reflects the spatial and velocity distribution of ions above the target surface. For acceptable signal to noise ratios, all mass spectra in the present experiment were obtained by a cumulative collection of 300 laser shots.

3. Results and discussion

The signals due to ionic products created directly from the graphite surface can be detected above the laser fluence of 0.5 J/cm². In order to investigate the plume composition in our experimental condition, we report in Fig. 2 the typical TOF mass spectra of carbon cluster ions obtained from 355 nm laser irradiation of a graphite target in high-vacuum conditions at two laser fluences. The spectra are measured in a mass spectrometer mode ($\tau_d = 0$ μ s). At 0.5 J/cm² laser fluence, the spectrum mostly consists of the C_n^+ ions with $n = 1, 3, 5, 7, 11$, and 15 although the yield decreases rather monotonically as the cluster

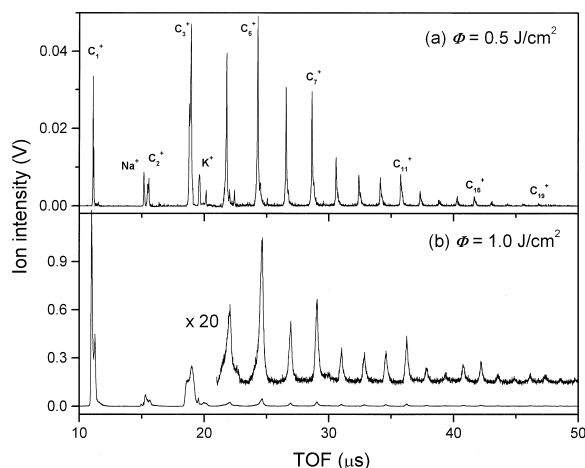


Fig. 2. Typical TOF mass spectra of laser ablated ions produced by laser irradiation ($\lambda = 355$ nm) of a graphite target in high vacuum. The spectra are obtained at laser fluences of (a) $\Phi = 0.5$ J/cm², and (b) $\Phi = 1.0$ J/cm².

size increases. Even-numbered peaks were found to be less abundant. The preferential formation of odd-numbered cluster ions has also been reported in the previous mass spectra on carbon clusters generated by $\lambda = 266$ and 532 nm laser vaporization [13,14].

It is found that the dependence of the mass distribution on the laser fluence changes drastically. The relative enhancement of the C_1^+ and C_3^+ ion signals becomes prominent at a high laser fluence of 1.0 J/cm². A similar tendency has also been found in a recent study on the laser ablation of graphite at 266 nm [15], in which the dominant species consist of C_1^+ and C_3^+ ions as increasing the laser fluence. This is consistent with the view that the concentration of the small cluster ions increases with laser fluence mainly because of the fragmentation of larger clusters within the hot plume. The broad temporal distribution of each cluster peak as compared with the results at low laser fluence [see Fig. 1(a)] also supports the high kinetic energy of cluster ions. In our experiments, we have no direct method for determining whether the fragment ions are the result of neutral fragmentation followed by ionization or direct fragmentation of parent ions as the result of absorption of excess laser photons. However, the fact that direct ionization dominates at low fluence whereas fragmentation dom-

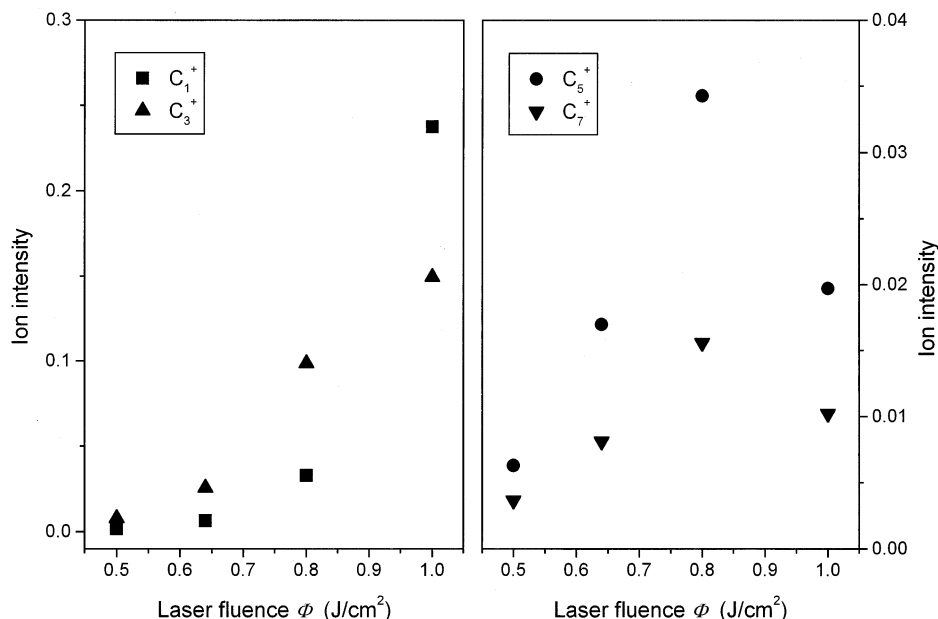


Fig. 3. Intensity plot of C_n^+ ($n = 1, 3, 5$, and 7) ions at different laser fluences.

inates at high fluence would seem to indicate that the dissociation occurs after formation of the parent ions.

According to the studies on a liquid phase of carbon by Dresselhaus and coworkers [16,17], the hot particles with a certain size have strongly been suggested to be emitted from the hot surface (>4000 K) immediately following the nanosecond laser irradiation with several hundred mJ/cm^2 [17]. These hot particles may spontaneously dissociate into small carbon clusters because they are reasonably supposed to have enough internal energy. During these processes, the bond breaking and/or energy release by translation of the fragments should effectively play a role as a major cooling process for the hot particles. Therefore, the intensity dependence of C_n^+ ions on laser fluence in the present experiment gives a conclusion that at low laser fluence the ablated C_n^+ ions are formed directly from the graphite surface, but the fragmentation of large clusters contributes a significant role in increasing the laser fluence.

In order to understand the formation mechanism of carbon cluster ions, C_n^+ intensities ($n = 1, 3, 5$, and 7) are plotted against laser fluence. The ion signal of each species is obtained by integration of the corre-

sponding TOF spectrum. Fig. 3 shows that the intensities of C_1^+ and C_3^+ ions increase quite substantially with laser fluence, whereas those of C_5^+ and C_7^+ ions exhibit a maximum at $0.8 \text{ J}/\text{cm}^2$. The decreased intensities of C_5^+ and C_7^+ ions at high laser fluence clearly reveal that these ions undergo fragmentation into the small cluster ions because of their high internal energies, as mentioned above. The nonlinear intensity dependence of C_n^+ ions on laser fluence can be described by the following equation

$$I = a\Phi^q \quad (1)$$

where I is the integrated C_n^+ signal, a is a constant, and Φ is the laser fluence. Because the power law is characteristic for a multiphoton process, we consider that the ablation of C_n^+ ions is caused by the q photon process at a low laser fluence of less than $\sim 0.9 \text{ J}/\text{cm}^2$ when $\lambda = 355 \text{ nm}$ is used as the light source. The q values are determined from the slopes of the $\log I$ versus $\log \Phi$ plots before attaining the maximum for each C_n^+ (see Table 1). The values of q for C_1^+ , C_3^+ , C_5^+ , and C_7^+ were 6.5, 5.6, 3.8, and 3.2, respectively. Considering the 355 nm excitation wavelength ($h\nu =$

Table 1

Theoretical and experimental q values for C_n^+ cluster ions at 355 nm wavelength^a

C_n^+	C_1^+	C_3^+	C_5^+	C_7^+
$(2n + 1)$	3	7	11	15
$E_d(nC)$	7.4	17.3	27.1	37.0
$E_f(C_n)^b$	0	−12.7	−23.9	−35.2
$IP(C_n)^b$	11.0	11.4	10.7	10.0
$E(C_n^+)$	18.4	16.0	13.9	11.8
q_{theory}	5.3	4.6	4.0	3.4
q_{exp}	6.5	5.6	3.8	3.2

^a Units of $E_d(nC)$, $E_f(C_n)$, $IP(C_n)$, and $E(C_n^+)$ are in eV.^b [18].

3.5 eV), the observed multiphoton energies are much higher than the ionization potentials of carbon clusters (10.0–11.4 eV) [18].

The number of photons, q , necessary for generating C_n^+ ions can be estimated by the energy $E(C_n^+)$ needed to produce C_n^+ from a graphite surface. In order to calculate $E(C_n^+)$, the following relation is used [14],

$$E(C_n^+) = E_d(nC) + E_f(C_n) + IP(C_n) \quad (2)$$

where $E_d(nC)$ is the bond-dissociation energy necessary to form neighboring n carbon atoms in the graphite structure; $E_f(C_n)$ is the formation (or stabilization) energy of the C_n cluster, and $IP(C_n)$ is the ionization potential for C_n . In order to produce a C_n cluster from an atomic monolayer in graphite composed of six-membered rings, the breaking of $2n + 1$ bonds should be involved. From the binding energy $E_d(C)$ of a carbon atom (7.4 eV) in the graphite [19], $E_d(nC)$ can be represented by Eq. (3)

$$E_d(nC) = E_d(C)(2n + 1)/3 \quad (3)$$

Assuming that the incident photon is completely converted into thermal energy, the theoretical number of photons necessary to overcome $E(C_n^+)$ energy can be determined, as summarized in Table 1. The calculated $E(C_n^+)$ value decreases with cluster size because of its stabilization energy, which results in a decrease of q with cluster size. The observed q values are in reasonable agreement with the theoretical values, indicating that laser ablation of graphite at $\lambda = 355$ nm occurs by the multiphoton energy. In studies on

the energetics of C_n^+ ions produced by laser ablation of graphite at $\lambda = 1064$, 532, and 266 nm, Gaumet et al. [14] have suggested that the C_n^+ ion formation at 1064 and 532 nm can be understood by the conversion of multiphoton energy into thermal energy whereas photoelectric excitation becomes important at 266 nm wavelength. The present results strongly suggest that at $\lambda = 355$ nm the cluster ions are formed as a result of the thermal process. Based on the above results, it is believed that during the initial stage of ablation the carbon clusters C_n^+ ($n = 1$ –20) are produced directly from the graphite surface, not by the aggregation of carbon atoms and small clusters.

To investigate the temporal evolution of an ablated plume, we employed the pulsed-field time-of-flight mass spectrometric technique, which observes the TOF ion signal as a function of the delay time between the laser shot and the repelling electric field, applied to the ion optics. The delay time is stepped to reveal the arrival time distribution of the ionic species in time. The different traces refer to different slices of the ablation plume as it expands in the vacuum. This method thus offers an excellent means to investigate the time-dependent velocity distribution of the ionic species during the initial stage of plume expansion. The TOF spectra corresponding to the C^+ ions were plotted as a function of the delay time, as shown in Fig. 4. The spectra were obtained with a laser pulse energy of 0.8 J/cm². After 0.06 μ s, each TOF spectrum consists of two components as a result of the two separated ionic clouds. An increase in the delay time results in a monotonic decrease of ion intensity as

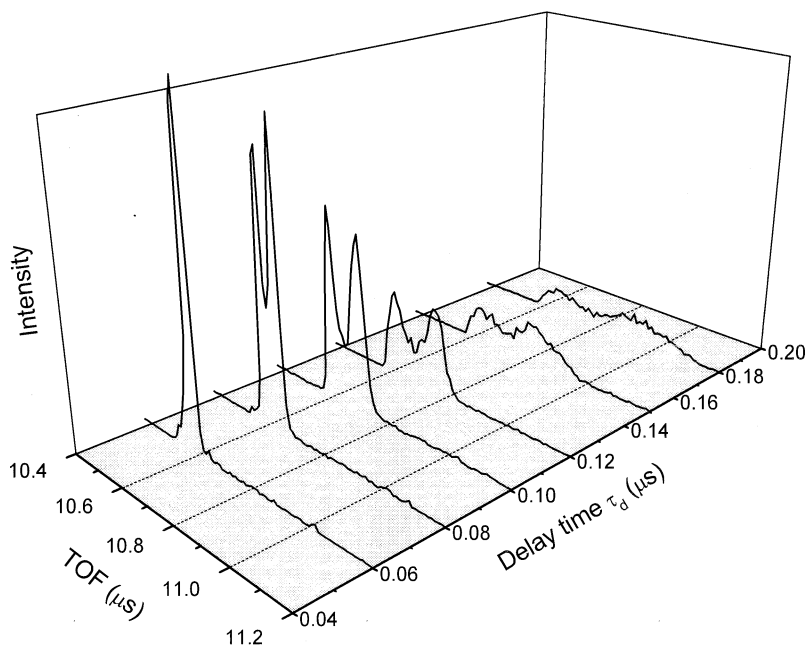


Fig. 4. TOF spectra of laser ablated C^+ ions in high vacuum as a function of delay time between the laser shot and the extraction pulse: extraction zone distance is 10 mm. The ions were ablated by 355 nm with a pulse energy of 0.8 J/cm^2 .

well as the broad temporal distribution of each peak. These observations, as expected, indicate that the ablated plume spreads in space above the target surface during the delay time after the laser irradiation. The arrival time of each component shifts to a longer flight time with increasing τ_d because the ions move away from the target surface during τ_d , thus acquiring less kinetic energy U after repelling electric field. For this reason, the arrival time of the fast velocity component is longer than that of the slow one in each spectrum, as will be described in more detail later.

The twin peak structure of C^+ ions can be assigned because of the occurrence of species corresponding to those generated by the dissociation of higher clusters, giving rise to the slower velocity component and to those generated by a direct ablation process giving rise to the fast peak. But this is not likely because single peak distribution is not observed, even at low laser fluence where the minor contribution of the fragmentation process is expected. Another possible explanation could be the collision-induced ionization

[20] in the later stages of the expanding ablation cloud, resulting in the small, shoulder contribution of the slow ions. However, the collision-induced ionization probability is expected to be very low in the present experiments with low laser fluence and in high vacuum conditions.

In a recent study on the CO_2 and excimer laser ablations of the Ti target, Metev et al. [21] have observed the two different temporal shapes of the ion current pulse in the plasma probed using a modified quadrupole mass spectrometer. The observation of two components in the propagation of the ablated plume has also been reported before using fast intensified-CCD photography of YBCO laser ablation [22,23]. These features are in reasonable agreement with our current observations. The collisions between the ejecta during the initial expansion are theorized to result in a Knudsen layer or unsteady adiabatic expansion zone that produces a stopped or backward-moving component close to the target and a strongly forward-peaked velocity component away from the target [24,25]. This phenomenon is also consistent

with the view that there is ample time for the particles to undergo collisions within the plume during the nanosecond laser pulse. This tends to accelerate the motion of the ions at the front side of the plume, and consequently, slow down the ions that ablate near the end of the laser pulse. It is, therefore, concluded that the particles emitted on the surface of the target are separated into two components at the early stage of the ablation.

The TOF distributions give the arrival time of ions at a certain point in space with a known flight length and these can easily be transformed into velocity distribution. In order to get a more clear evaluation of the velocity component v_z of the ions at directions normal to the ablation surface, we employed the shifted Maxwell–Boltzmann (MB) distribution to fit our TOF data. For the bimodal distributions that we observe the fit function is of the form [26]

$$f(v_z) = Av_z^3 \exp[-m(v_z - v_s)^2/2kT_s] + Bv_z^3 \exp[-m(v_z - v_f)^2/2kT_f] \quad (4)$$

where $v_{s,f}$ denote the flow velocities and $T_{s,f}$ the translational (or stream) temperatures for the slow and fast components, respectively, m is the mass number of species, k is the Boltzmann constant, and A and B are parameters used to fit the relative intensities of the two components.

Following a delay time τ_d after the laser shot, the TOF in the laboratory frame of an ablated ion is dependent on the component of the initial velocity of the ions along the detection axis as well as acceleration because of the electric field, E_a . For an ablated ion of the mass m and the charge q , the kinetic energy U after acceleration is given by

$$U = qE_a(s_o - v_z\tau_d) + U_z \quad (5)$$

where s_o is the distance between the repelling and collecting electrodes. The first term is the acquired energy of an ablated ion by E_a after the delay time τ_d . U_z is the initial kinetic energy of the ablated ion prior to acceleration, which is dependent on the initial velocity v_z . Thus, the TOF of the ion with respect to the onset of the acceleration voltage is given by the

sum of the flight times spent in the acceleration (T_a) and field-free drift regions (T_f)

$$\text{TOF}(v_z\tau_d, U_z) = (2m)^{1/2}(qE_a)^{-1}(U^{1/2} - U_z^{1/2}) + (m/2)^{1/2}D_fU^{-1/2} \quad (6)$$

where D_f is the distance of the field-free drift region. From the measured TOF distribution $I(t)$ of ablated ions, the velocity distribution is determined by the following relation

$$I(\text{TOF})d\text{TOF} = f(v_z)dv_z \quad (7)$$

In these fittings, it is assumed that the initial velocity distribution of an ablated ion remains constant during the delay time. Although the estimated velocity distribution $f(v_z)$ includes the instrumental resolution factor of TOFMS, its flow velocity of an ablated ion can be precisely obtained from the experimental data and Eq. (7). Here flow velocities $v_{s,f}$ and stream temperatures $T_{s,f}$ are used as adjustable parameters.

Fig. 5 shows the results of the best curve fit (closed circles) and experimental TOF spectra (solid lines) of a C^+ ion with a laser fluence of 0.8 J/cm^2 at $\tau_d = 0.08$ and $0.12 \mu\text{s}$. The errors of flow velocities are found to be in the range of $\pm 20 \text{ m/s}$. Each peak in the TOF spectra is well fitted by a shifted MB distribution of ejected ions given in Eq. (4), implying that the ions desorbed by the laser ablation reach thermal equilibrium. Such thermal equilibrium results from many collisions between ions because the ion density is very high at the early stage of the ion flight. The fast and slow flow velocities at $\tau_d = 0.08 \mu\text{s}$ are determined to be 1800 m/s and 300 m/s , respectively. At $\tau_d = 0.12 \mu\text{s}$, the fast velocity in the plume is increased to 2900 m/s . The results indicate that the expansion process of fast ionic species in the plume is similar to that of the supersonic nozzle expansion [27].

The time resolved observation presented here characterizes the axial expansion of the plume, i.e. strictly along a direction perpendicular to the target surface. The flow velocities $v_{s,f}$ of C^+ ions, plotted as a function of delay time at a laser fluence of 0.8 J/cm^2 , are represented in Fig. 6. The observation of $v_f \sim 3500 \text{ m/s}$ at a long delay time is in agreement with the result by Kokai et al. [15]. It is quite interesting to

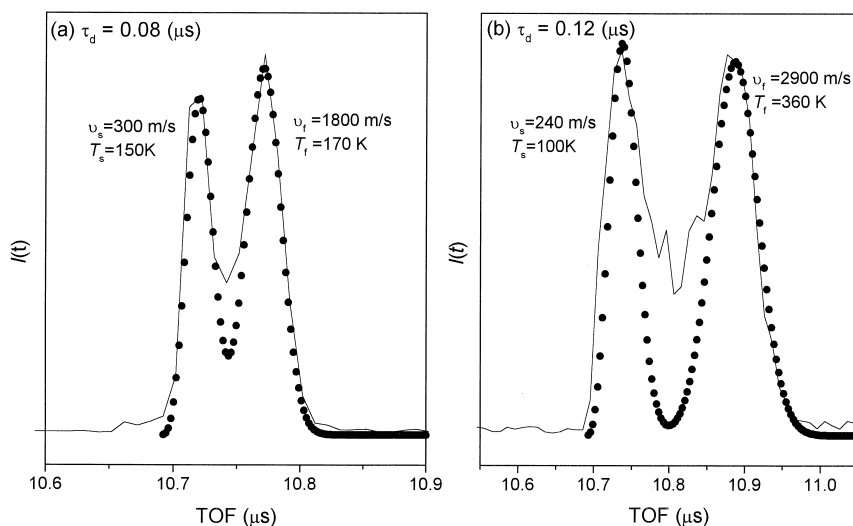


Fig. 5. The shifted Maxwell–Boltzmann fit of the TOF spectra of a C^+ ion with a laser fluence of 0.8 J/cm^2 at (a) $\tau_d = 0.08$, and (b) $\tau_d = 0.12 \text{ } \mu\text{s}$. The solid lines are experimental data and the closed circles are the best fit. Fit parameters (a) $T_s = 150 \text{ K}$, $v_s = 300 \text{ m/s}$, $T_f = 170 \text{ K}$, $v_f = 1800 \text{ m/s}$, (b) $T_s = 100 \text{ K}$, $v_s = 240 \text{ m/s}$, $T_f = 360 \text{ K}$, $v_f = 2900 \text{ m/s}$.

note that the flow velocity of a fast component increases rapidly with delay time, showing a free expansion behavior, and reaches a plateau ($v_f = 3000\text{--}3500 \text{ m/s}$) after $\tau_d = 0.12 \text{ } \mu\text{s}$. The increase in the fast velocity component after the laser irradiation can be a result of the hydrodynamic effects of the plume formed above the target surface. Initially, the expansion is isothermal during the time interval of the

laser pulse. After the laser pulse terminates, the plasma expands adiabatically in the vacuum and the thermal energy of the plasma is converted into kinetic energy. The plasma cools rapidly and the stream velocity starts to increase. On the other hand, the slow velocity component (less than 500 m/s) remains almost unchanged. This slow-moving component is presumably due to the fact that the ions ablated near the end of the nanosecond laser pulse are decelerated via collisions and/or Coulomb interactions inside the dense plume, but a complete understanding awaits a further study.

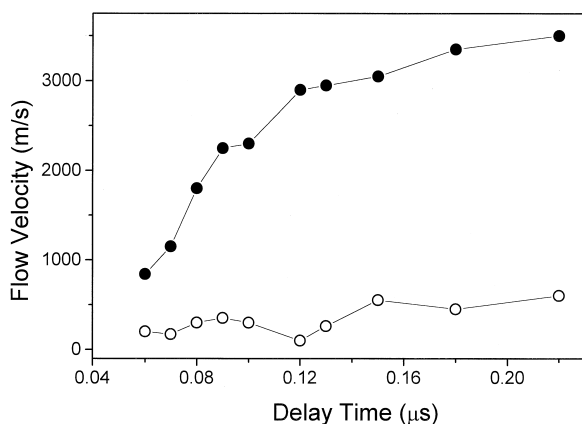


Fig. 6. The flow velocity of C^+ ions as a function of delay time between the laser irradiation and the extraction pulse at 0.8 J/cm^2 laser fluence.

4. Conclusion

Laser ablation of a graphite target at 355 nm has been investigated by a TOF mass spectrometer. A strong nonlinear dependence of the amount of C_n^+ ions on laser fluence is interpreted by the mechanism that C_n^+ ions are produced directly from the surface via conversion of the multiphoton energy into the thermal energy. The pulsed-field technique was used to characterize the temporal evolution of C^+ ions in a laser-ablated plume. The TOF distributions of C^+

ions are simulated very well by shifted Maxwell–Boltzmann distributions superimposed on a flow velocity. The time resolved analysis of the ablated ions shows the two velocity distributions with the fast and slow components, indicating that the ejecta emitted above the target surface separates into two components during plume propagation. In conclusion, we believe that pulsed-field time-of-flight mass spectrometry is one of the most suitable ways for the direct measurement of ion energies, which is of great interest for laser plume characterization in a number of important applications.

Acknowledgements

The authors gratefully acknowledge the Korea Research Foundation (Grant No. 1998-015-D00140) and Wonkwang University for support of this research in 1998. One of the authors (H.-S. Im) also greatly appreciates partial support from the Ministry of Science and Technology.

References

- [1] A.W. Johnson, T.W. Sigmon, G. L. Loper (Eds.), *Proceedings of the Material Research Society Symposia*, 1989, p. 129.
- [2] H.W. Kroto, R.J. Heath, S.C. Brien, R.F. Curl, R.E. Smalley, *Nature* 318 (1985) 162.
- [3] S. Iijima, T. Ichihashi, *Nature* 363 (1993) 603.
- [4] D.H. Lowndes, D.B. Geohegan, A.A. Puretzky, D.P. Norton, C.M. Rouleau, *Science* 273 (1996) 898.
- [5] R.E. Smalley, *Acc. Chem. Res.* 25 (1992) 98.
- [6] L.A. Bloomfield, M.E. Geusic, R.R. Freeman, W.L. Brown, *Chem. Phys. Lett.* 121 (1985) 33.
- [7] D.M. Cox, K.C. Reichmann, A. Kaldor, *J. Chem. Phys.* 88 (1988) 1588.
- [8] K. Kaizu, M. Kohno, S. Suzuki, H. Shiromaru, T. Moriwaki, Y. Achiba, *J. Chem. Phys.* 106 (1997) 9954.
- [9] T. Moriwaki, K. Kobayashi, M. Osaka, M. Ohara, H. Shiromaru, Y. Achiba, *J. Chem. Phys.* 107 (1997) 8927.
- [10] H.-S. Im, S.-H. Kim, Y.-K. Choi, K.H. Lee, K.-W. Jung, *Bull. Korean Chem. Soc.* 18 (1997) 56.
- [11] Y.-K. Choi, H.-S. Im, K.-W. Jung, *Bull. Korean Chem. Soc.* 19 (1998) 830.
- [12] Y.-K. Choi, H.-S. Im, K.-W. Jung, (unpublished).
- [13] E.A. Rohlfing, D.M. Cox, A. Kaldor, *J. Chem. Phys.* 81 (1984) 3322.
- [14] J.J. Gaumet, A. Wakisaka, Y. Shimizu, Y. Tamori, *J. Chem. Soc., Faraday Trans.* 89 (1993) 1667.
- [15] F. Kokai, Y. Koka, *Nucl. Instrum. Methods Phys. Res. B* 121 (1997) 387.
- [16] J. Steinbech, G. Braunstein, M.S. Dresselhaus, T. Venkatesan, D.C. Jacobson, *J. Appl. Phys.* 58 (1985) 4374.
- [17] J. Heremans, C.H. Olk, G.L. Eesley, J. Steinbech, G. Dresselhaus, *Phys. Rev. Lett.* 60 (1988) 452.
- [18] R. Raghavachari, J.S. Binkley, *J. Chem. Phys.* 87 (1987) 2191.
- [19] T.W. Ebbesen, *Carbon Nanotubes: Preparation and Properties*, CRC, New York, 1997.
- [20] J. Dieleman, E. van de Riet, J.C.S. Kools, *Jpn. J. Appl. Phys.* 31 (1992) 1964.
- [21] S. Metev, M. Ozegowski, G. Sepold, S. Burmester, *Appl. Surf. Sci.* 96–98 (1996) 122.
- [22] D.B. Geohegan, *Appl. Phys. Lett.* 60 (1992) 2732.
- [23] D.B. Geohegan, in E. Fogarassy, S. Lazare (Eds.), *Laser Ablation of Electronic Materials: Basic Mechanisms and Applications*, North-Holland, Amsterdam, 1992, pp. 73–88.
- [24] R. Kelly, B. Braren, *Appl. Phys. B: Photophys. Laser Chem.* 53 (1991) 160.
- [25] R. Kelly, *J. Chem. Phys.* 92 (1990) 5047.
- [26] J.P. Zheng, Z.Q. Huang, D.T. Shaw, H.S. Kwok, *Appl. Phys. Lett.* 53 (1988) 534.
- [27] J.B. Anderson, R.P. Andres, J.B. Fenn, *Adv. Chem. Phys.* 10 (1966) 275.